Supplemental figures (Martinic et al)

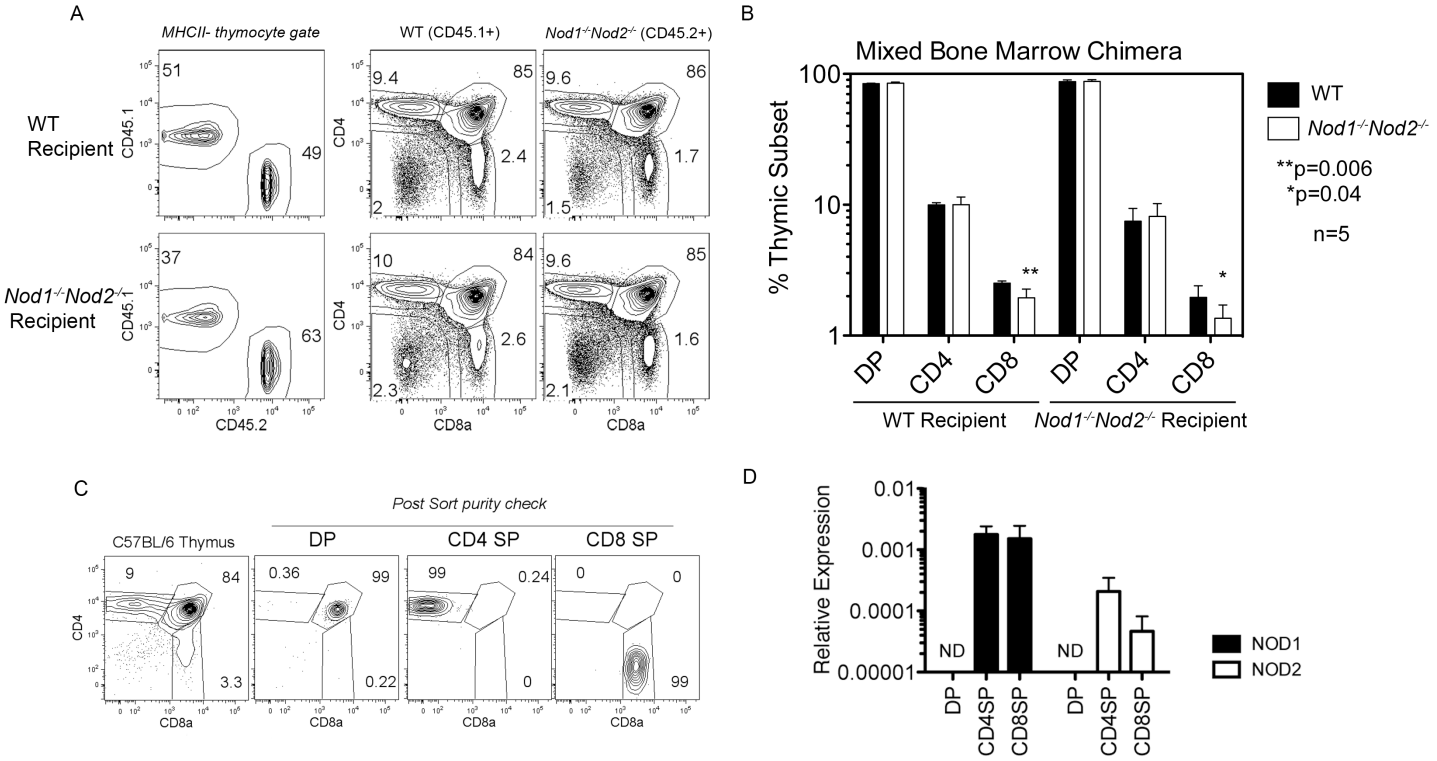

Supplementary Figure 1. Decreased CD8 SP thymocyte population in *Nod1$^{-/-}$Nod2$^{-/-}$* mice is T cell intrinsic. Mixed bone marrow chimeras were generated by injecting a 1:1 ratio of T-depleted B6.SJL-Ptprc^{a}Pepc^{b} (WT, CD45.1^{+}) and *Nod1$^{-/-}$Nod2$^{-/-}$* (CD45.2^{+}) bone marrow into lethally irradiated WT or *Nod1$^{-/-}$Nod2$^{-/-}$* recipients. Nine weeks after injection, the donor thymocyte population in the different recipients was analyzed. **(A)** Representative flow cytometry plots from the thymus of WT (upper row) and *Nod1$^{-/-}$Nod2$^{-/-}$* (lower row) bone marrow recipients. First column shows frequency of WT (CD45.1^{+}) and *Nod1$^{-/-}$Nod2$^{-/-}$* (CD45.2^{+}) donor cells in the thymus of WT and *Nod1$^{-/-}$Nod2$^{-/-}$* recipients after gating on MHCII^{-} cells. Second and third columns represent frequency of WT donor and *Nod1$^{-/-}$Nod2$^{-/-}$* donor thymocyte populations, respectively, in WT (upper row) and *Nod1$^{-/-}$Nod2$^{-/-}$* recipients (lower row).

(B) Frequency of WT (black) and *Nod1$^{-/-}$Nod2$^{-/-}$* (white) donor thymocyte subsets in WT (left) and *Nod1$^{-/-}$Nod2$^{-/-}$* (right) recipients. Bars represent the mean, error bars represent the SD. Statistical analysis with unpaired t tests was performed. Data represent pooled results from two independent experiments with a total of 5 mice per group analyzed.

(C,D) Expression of NOD1 and NOD2 in thymocyte subsets. **(C)** C57BL/6 thymocytes were sorted on a BD Aria using CD4 and CD8 markers to generate either DP (CD4+CD8+), CD4 SP (CD4+CD8-) or CD8 SP (CD8+CD4-) subsets. cDNA was generated from genomic DNA depleted RNA isolated from each subset and used as template for quantitative PCR analysis using NOD1 and NOD2 specific primers. **(D)** Relative Expression of each gene is shown relative to actin levels measured by Realtime PCR in each sample.

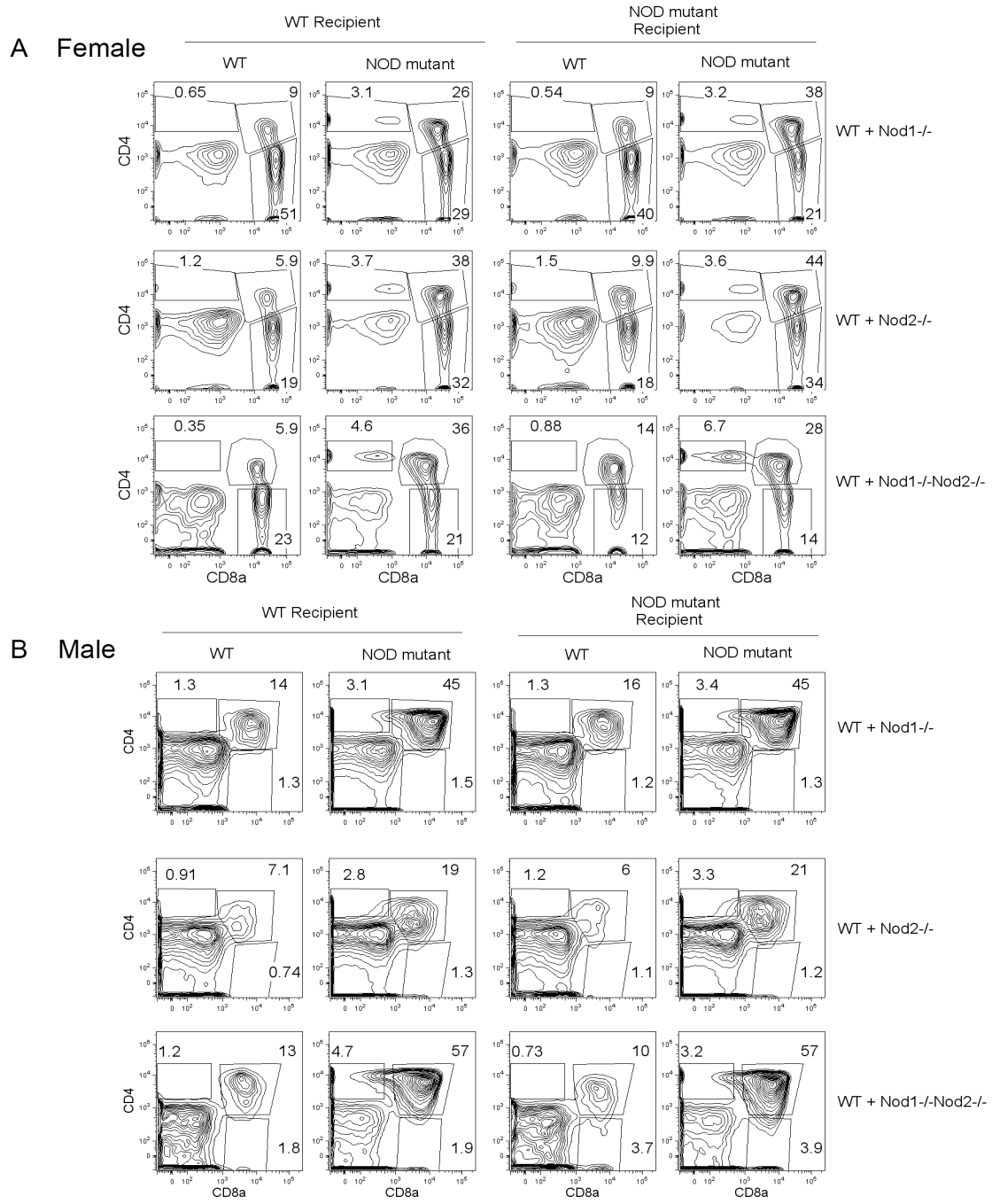

Supplementary Figure 2. Altered thymic selection in H-Y TCR Tg *Nod1*$^{-/-}$*Nod2*$^{-/-}$ thymocytes is T cell intrinsic. Mixed bone marrow chimeras were generated by injecting a 1:1 ratio of H-Y TCR Tg T-depleted B6.SJL-CD45.1 (WT, CD45.1^{+}) and NOD mutant (CD45.2^{+}) bone marrow into lethally irradiated non transgenic WT or NOD mutant female **(A)** and male **(B)** recipients. 6 weeks after injection, the donor thymocyte populations in each recipient were analyzed by gating on T3.70+ cells, then staining for CD45.1 and CD45.2. Representative flow cytometry plots of thymocytes of H-Y TCR Tg WT (left column) and NOD mutant (right column) origin, isolated from either WT (left two columns) or NOD mutant (right two columns) recipients. The different rows show the WT and *Nod1*$^{-/-}$ (upper row), WT and *Nod2*$^{-/-}$ (middle row), and WT and *Nod1*$^{-/-}$*Nod2*$^{-/-}$ (bottom row) donor thymocyte population in WT (left two columns) and NOD mutant (right two columns) bone marrow recipients. Numbers in plots represent percentages of depicted populations. Data are representative of four mice per group analyzed.

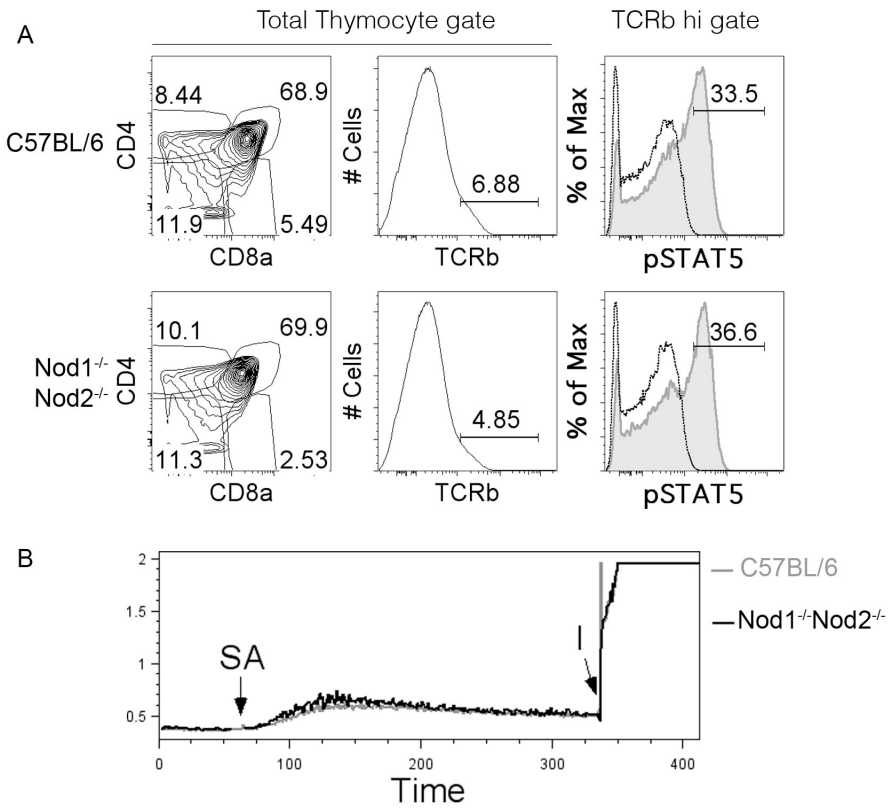

Supplementary Figure 3. *Nod1*$^{-/-}$*Nod2*$^{-/-}$ thymocytes show IL-7/STAT5 signaling and normal Ca^{2+} flux.

(A) Representative flow cytometry plots from C57BL/6 (upper row) and *Nod1*$^{-/-}$*Nod2*$^{-/-}$ (lower row) thymocytes. First column shows CD4 and CD8a staining of total thymocytes; second column shows histogram plots for the expression of TCRβ chains amongst all thymocytes; third column shows histogram plots gated on TCRβ^{hi} thymocytes and stained for phosphorylated STAT5 (pSTAT5) after culture with (filled) or without IL-7 (black line) for fifteen minutes.

(B) Representative store-operated Ca^{2+} influx in C57BL/6 (grey) and *Nod1*$^{-/-}$*Nod2*$^{-/-}$ (black) thymocytes stimulated by crosslinking of biotinylated anti-CD3 and anti-CD4 with streptavidin (SA), followed by the addition of ionomycin (I) (positive control). C57BL/6 cells were CFSE labeled, mixed at a 1:1 ratio with unlabeled *Nod1*$^{-/-}$*Nod2*$^{-/-}$ cells, incubated with the calcium indicator Indo-1-AM and assayed in one FACS tube. Ca^{2+} flux was measured by changes in the violet/blue fluorescence ratio of Indo-1-AM. A representative of two independent experiments is shown.

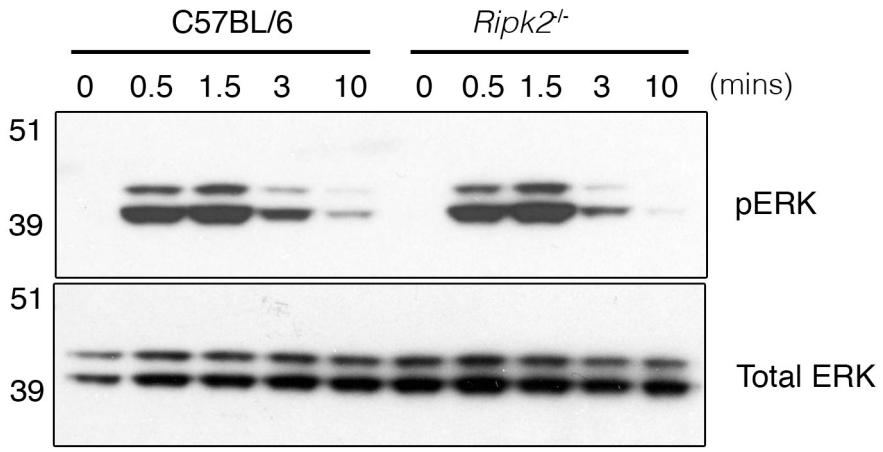

Supplementary Figure 4. *Ripk2* deficiency has no effect on TCR-mediated ERK activation. Immunoblot analysis of phosphorylated (pERK) and total ERK1/2 in lysates of rested or TCR-stimulated C57BL/6 (left) and *Ripk2*$^{-/-}$ (right) thymocytes. For TCR stimulation, thymocytes were bound with biotinylated anti-CD3 and anti-CD4 followed by stimulation with streptavidin over time (ten minutes). After pERK was detected, the membranes were stripped and re-probed with an antibody detecting total ERK1/2.